RESEARCH ARTICLE

ScienceAsia 49 (2023): **116–123**

doi: 10.2306/scienceasia1513-1874.2022.140

Selective catalytic hydrogenation of furfural to cyclopentanone over Ru-Co bimetallic catalyst

Wei Long[a,b,*], **Shousheng Huang**[c], **Yinfei Huang**[d]

[a] College of Chemistry, Guangdong University of Petrochemical Technology, Maoming 525000 China
[b] Guangdong Provincial Key Laboratory of Petrochemical Pollution Process and Control, Guangdong University of Petrochemical Technology, Maoming 525000 China
[c] College of Science, Guangdong University of Petrochemical Technology, Maoming 525000 China
[d] College of Mechanical and Electrical Engineering, Guangdong University of Petrochemical Technology, Maoming 525000 China

[*] Corresponding author, e-mail: longwei@gdupt.edu.cn

Received 19 Apr 2022, Accepted 4 Sep 2022
Available online 25 Oct 2022

ABSTRACT: The conversion of furfural to cyclopentanone over Ru-Co bimetallic catalysts was studied under a hydrogen atmosphere. It was found that furfural in water solution converted to cyclopentanone with high selectivity under 3.0 MPa and 433 K. Cyclopentanol and furfuryl alcohol were detected as by-products. Addition of cerium oxide greatly improved the catalytic performance. In the presence of 6%Ru-6%Co-6%CeO_2/MSEP catalyst, 100% furfural conversion and 71.35% selectivity to cyclopentanone were obtained successfully. The catalysts were characterized by BET, FT-IR, XRD, SEM, TEM, TG and Hydrogen chemisorption. Additionally, the catalyst successfully operated in 5 wt% furfural solution and displayed high stability.

KEYWORDS: furfural, cyclopentanone, hydrogenation, rearrangement

INTRODUCTION

Nowadays, renewable energy research is of vital importance due to the ever increasing demand for energy and diminishing petroleum reserves [1]. Biofuels are well recognized as potential alternatives in the transportation sector and should be implemented in the very near future [2]. Hence, the exploitation of biofuels is essential for our development [3]. Recently, newly discovered biofuels extracted from biomass conversion, have become a serious area of research [4–7].

Furfural is a key platform molecule in biomass conversion, and it is an important feedstock for the production of furfuryl alcohol, 2-methylfuran or cyclopentanone (CPO) [8]. In industry, furfural is produced from agricultural raw materials rich in pentosan, such as bagasse, oat hulls and corncobs [9]. Additionally, it is a very cheap renewable source, and can be converted into useful chemicals through polymerization, hydrogenation or oxidation reactions [10]. To-date, there have been numerous technological reports regarding furfural conversion [11–13].

CPO is an important chemical intermediate in the production of pharmaceuticals, insecticides and rubber chemicals, which is generated via decarboxylation of adipic acid or selective catalytic hydrogenation of furfural [14]. Both furfural and CPO have five carbon atoms, but such conversions are not easy and require the participation of hydrogen ions and polar solvent [15]. Water is a good polar solvent but the reaction temperature is limited. Catalytic hydrogenation can be performed at different reaction temperatures, and the activity of catalyst depends on reaction temperature [16].

Ni-Cu/SBA-15 bimetallic catalysts have been applied for the conversion of furfural to cyclopentanone under a hydrogen atmosphere, the opening and closing of the furan ring are closely related to the attack of the H_2O molecule at the 5-position of furfuryl alcohol [17]. The high selectivity to CPO is ascribed to the presence of 2-cyclopentenone. It was reported that 5%Pd-10%Cu/C bimetallic catalyst could be utilized for the highly selective rearrangement of furfural to CPO, where the best conversion rate was 98% and selectivity to CPO was 94.0% using only 1 wt% concentration of furfural in water solution [18]. When the Cu-Ni-Al hydrotalcites derived oxides were employed as catalysts, CPO yield was up to 95.8% when the reaction conditions were 413 K under H_2 pressure of 40 bar for 8 h [19]. Hronec and Fulajtarová [20] found that furfural dissolved in water was converted to CPO with high selectivity at temperatures above 413 K and H_2 pressures above 30 bar. The presence of 5% Pt/C catalyst produced 76.50% selectivity to CPO after 30 min at 433 K and H_2 pressure of 80 bar. Prolongation of the reaction time led to CPO hydrogenation to cyclopentanol. Hence, bimetallic catalysts are more suitable for the hydrogenation process of furfural to CPO and the water is the essential solvent.

Recent reports that examine furfural rearrangement provide various reasons for its occurrence, but no consensus evolved from the studies. Hronec et al [15] found the high selectivity of furfural rearrangement to CPO stemmed from the influence of the balance between the rates of formation of furfuryl alcohol polymers on the catalyst surface and their decomposition. The reaction was catalyzed by H^+ protons created by auto dissociation of water at certain temperatures and by acidic centers of catalyst. CuNi/Al-MCM-41 bimetallic catalyst afforded excellent catalytic performance in the tandem hydrogenation rearrangement of furfural to CPO in a near-neutral solution [21]. A small amount of Al highly dispersed in MCM-41 played an anchoring role and ensured the formation of highly dispersed CuNi bimetallic nanoparticles. The bimetallic synergy and charge transfer effects are the important factors to promote excellent catalytic performance, and the initial furfural concentration and the aqueous system's pH required precise control to minimize polymerization and achieve high selectivity to CPO. An efficient and economical multifunctional porous Co-400 catalyst was prepared for the furfural rearrangement to cyclopentanol [22]. The highly dispersed Co^0 species and amorphous porous Co_3O_4 species were key factors influencing high activity and chemoselectivity to the catalysts, which were precisely controlled at lower temperature. $Pd/NiMoO_4$ catalysts possess low Pd loading (1.0 wt%) and different Pd dispersion, they are capable of promoting the transformation of bioderived furfurals to CPO. The difference in catalytic performance stemmed from alterations to the adsorption configurations of the reactants and the transformation of Lewis acid sites to Brønsted acid sites by hydrogen spillover [23]. The hydrogenation active sites and acidic sites of the catalysts were adjusted by a water-mediated hydrogen spillover process, which were the key factors for the selectivity to CPO or cyclopentanols. Hence, for dispersed metal species, the hydrogenation active and acidic sites of the catalysts are potential influencing aspects of furfural rearrangement to CPO.

In this work, the selective catalytic hydrogenation process of furfural was examined, as shown in Scheme 1. The reaction utilized furfural as the raw material to produce CPO as the main product and cyclopentanol and furfuryl alcohol as by-products. Minor or rare by-products included tetrahydro furfuryl alcohol, 1,2-pentanediol, 1,4-pentanediol, 1,2-cyclopentanediol and 1,3-cyclopentanediol, and were dictated by the reaction conditions and catalysts employed. Modified sepiolite (MSEP) is very mysterious material for the catalytic hydrogenation in our former research [24]. In this study, MSEP was chosen as the catalyst support allowing the formation of Ru-Co bimetallic catalysts, which were used in the catalytic hydrogenation of furfural to CPO. Cerium oxide (CeO_2) as the assistant and its function in this reaction system also was investigated. The presented study describes a new route for efficient and cost effective synthesis of CPO via hydrogenation of furfural solution.

MATERIALS AND METHODS

Materials

Sepiolite (silicon dioxide, 42.20%; magnesium oxide, 20.66%; calcium oxide 18.75%; iron oxide, 0.30%; aluminum oxide, 0.26%; potassium oxide, 0.17%; manganese dioxide, 0.09% and sodium oxide, 0.07%) was purchased from Yuanyuan Sepiolite Ltd., Co. (Hunan, China). Analytical grade $RuCl_3 \cdot 3\,H_2O$, $Co(NO_3)_3 \cdot 6\,H_2O$ and $Ce(NO_3)_3 \cdot 6\,H_2O$ were purchased from Sigma Aldrich (Guangdong, China). Furfural, hydrochloric acid, and ammonia water were from Sinopharm Chemical Reagent Ltd., Co. (Shanghai, China). Furfural was purified by distillation and stored at 258 K. Hydrogen gas (99.99%) was purchased from Changda gas Ltd., Co. (Guangdong, China).

Catalyst preparation

The modified sepiolite (MSEP) was prepared as the same method in the literature [24]. Ru/MSEP catalysts were prepared by typical wet impregnation method, MSEP solid was impregnated in ruthenium chloride ($RuCl_3 \cdot 3\,H_2O$) aqueous solution for 8 h. Then the mixture was dried at 393 K overnight and subsequently continuous calcined in nitrogen stream at 773 K for 6 h with a heating rate of 3 K/min. After cool down to room temperature, it was reduced under a stream of pure H_2 (100 ml/min) at 723 K for 2 h. Co/MSEP and Ru-Co/MSEP catalysts also were prepared by same method of Ru/MSEP, but the addition agent were $Co(NO_3)_3 \cdot 6\,H_2O$.

$Co\text{-}CeO_2$/MSEP and $Ru\text{-}Co\text{-}CeO_2$/MSEP catalysts were prepared by mixing and co-impreg nation method successfully. A certain amount of $Ce(NO_3)_3 \cdot 6\,H_2O$ was dissolved in 30 ml distilled water at 293 K, the predetermined amount of $RuCl_3 \cdot 3\,H_2O$ or $Co(NO_3)_3 \cdot 6\,H_2O$ was added. Then, A certain amount of ammonia water was added and stirring for 3 h. The MSEP was continuous impregnated in the above mixture for 8 h. Then the mixture was continuous dried at 393 K overnight and subsequently calcined in nitrogen stream at 773 K for 6 h with a heating rate of 3 K/min. The solid sample was reduced under a stream of pure H_2 (100 ml/min) at 723 K for 2 h. The letter x, y and z in $x\text{Ru-}y\text{Co-}z\text{CeO}_2$/MSEP represents the mass ratio of ruthenium, cobalt and ceric oxide, respectively.

Catalytic tests

Catalytic hydrogenation of furfural was performed in a 20 ml Teflon-lined stainless steel autoclave with a magnetic stirrer, an electric temperature controller. The reactant solution (20 g of 5 wt% furfural aqueous solution) and the certain amount of catalyst were mixed. The reactor was sealed and purged with H_2 to exclude air for six times, and subsequently it was pressurized

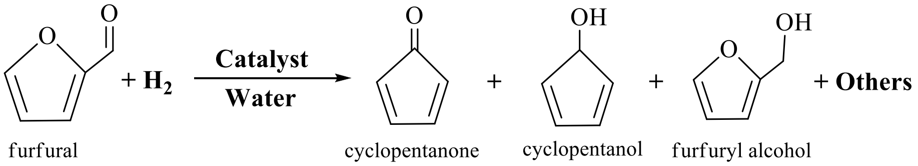

Scheme 1: Hydrogenation process of furfural. "Others" refers to minor by-products such as tetrahydro furfuryl alcohol, 1,2-pentanediol, 1,4-pentanediol, 1,2-cyclopentanediol and 1,3-cyclopentanediol.

to the definite pressure with H_2 under vigorous stirring after the required temperature reached.

After the reaction, the catalysts were separated by filtration from the liquid phase products. The quantitative determination of the liquid products was done by the external standard method using GC/MS analysis. After the liquid phase products were analyzed accurately, the content of the major products were determined by gas chromatography(7890 A, Agilent Technologies, USA) equipped with a HP-1, 50 m × 0.2 mm capillary column and a flame ionization detector (FID). The liquid phase products include cyclopentanone, cyclopentanol, furfuryl alcohol, tetrahydro furfuryl alcohol, 1,2-pentanediol, 1,4-pentanediol, 1,2-cyclopentanediol and 1,3-cyclopentanediol. The conversion of furfural and the selectivity to the products were calculated by the following equations [17].

$$\text{Conversion} = \left(1 - \frac{\text{Moles of furfural}}{\text{Moles of furfural loaded initially}}\right) \times 100\%$$

$$\text{Selectivity to product} = \frac{\text{Moles of product}}{\text{Moles of furfural converted}} \times 100\%$$

Catalyst characterization

The Brunauer-Emmett-Teller (BET) characterization of the samples were obtained by the nitrogen adsorption-desorption on a Quantachrome NOVA-2200E automated gas sorption system and the specific surface areas and pore size distributions were calculated. FT-IR spectra of the samples were recorded on a Nicolet 380 spectrometer with the wave number range of 400–4000 cm^{-1}. XRD patterns were determined under a D/max 2500TC diffractometer using Cu Kα radiation (λ=1.54 Å) and the tube voltage was 40 kV, the current was 30 mA. The pyridine adsorbed FT-IR spectra of the samples were recorded on a Nicolet iS™10 spectrometer. The morphologies of the samples were observed carefully with SEM on the JEOL JSM-7610LV scanning microscope operating with the accelerating voltage of 5 kV. The microstructure of the samples also was observed carefully by transmission electron microscopy (TEM) on the Tecnai G221 STelectron microscope working more than 180 kV. Hydrogen chemisorption was measured by using Quantachrome ChemBET 3000 instrument. The hydrogen chemisorption was performed at 333 K, and the hydrogen pulses (0.02 ml) were injected until the eluted areas of consecutive pulsed became constant. The thermal stability of the samples was analyzed by Netzsch 209C thermogravimetric (TG) with a temperature range of 50–700 °C, and a heating rate of 10 °C/min under nitrogen atmosphere.

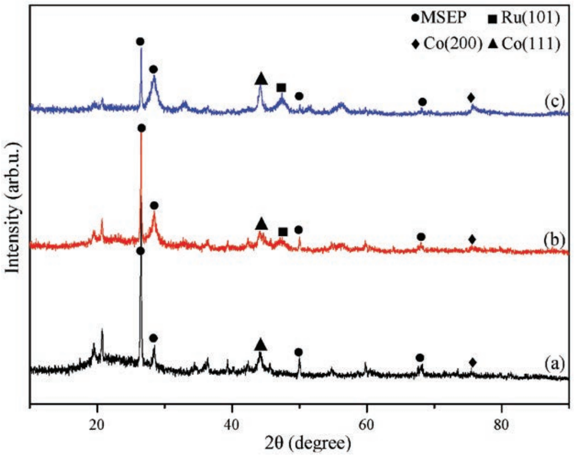

Fig. 1 X-ray diffraction (XRD) patterns of different samples. (a) 6%Co-6%CeO_2/MSEP, (b) 6%Ru-6%Co/MSEP, (c) 6%Ru-6%Co-6%CeO_2/MSEP.

RESULTS AND DISCUSSION

Characterization of catalyst

The textural properties of different samples are shown in Table 1. When the ruthenium, cobalt metal and ceric oxide were loaded onto the MSEP, the textural properties of catalysts differ. BET surface area of 6%Ru-6%Co-6%CeO_2/MSEP catalyst had a minimum of 98.6 m^2/g due to many species loaded onto the surface of MSEP, but the pore volume remained unchanged. The average pore sizes decreased 0.7 nm after the ceric oxide was added.

It was observed that all samples showed typical type I isotherms with sharp capillary condensation steps at the relative pressure (p/p_0) of 0.8–1.0 (Fig. S1), but this step shifted to a relative pressure (p/p_0) of 0.7–0.9 after the addition of CeO_2 species which is consistent with literature results [24]. According to the IUPAC classification, all the hysteresis loops are of type H4 with slit-shaped pores, and no N_2 adsorption platform is present in all samples from Fig. S1. Therefore, the pore structure of studied catalysts was

Table 1 Textural properties of different samples.

Catalyst	BET surface area (m^2/g)	Pore volume (ml/g)	Average pore size (nm)
6%Co-6%CeO_2/MSEP	100.3	0.24	10.5
6%Ru-6%Co/MSEP	101.3	0.24	10.5
6%Ru-6%Co-6%CeO_2/MSEP	98.6	0.23	9.8

Table 2 Hydrogen chemisorption data of some different catalysts.

Catalyst	H_2 uptake (μmol/g)	Metal surface area (m^2/g)	Dispersion (%)
6%Co/MSEP	35.4	14.5	3.2
6%Co-6%CeO_2/MSEP	51.6	23.1	6.7
6%Ru/MSEP	161.7	103.4	8.9
6%Ru-6%CeO_2/MSEP	181.3	117.6	11.3
6%Ru-6%Co/MSEP	210.8	135.9	16.6
6%Ru-6%Co-6%CeO_2/MSEP	241.9	159.7	22.7

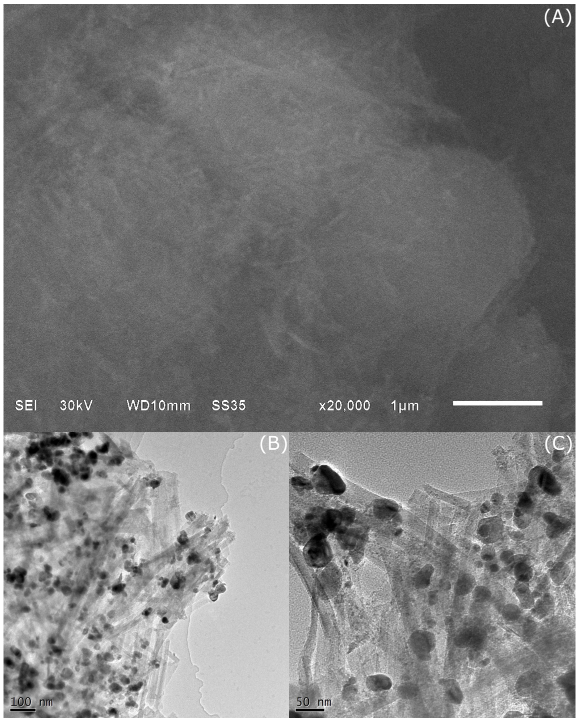

Fig. 2 SEM and TEM images of 6%Ru-6%Co-6CeO_2/MSEP catalyst, at magnification of (a) 20,000, (b) 200,000, and (c) 400,000.

not ordered and the addition of CeO_2 did not change the pore structure.

The Barrett-Joyner-Halenda (BJH) pore size distributions of different samples are shown in Fig. S2. The results showed that there were considerably more micropore structures on the surface of catalysts. However, a large change in pore size was observed upon addition of CeO_2 where the pore size of 6%Ru-6%Co-6%CeO_2/MSEP catalyst was 4.0–5.0 nm. Additionally, in the case of 6%Ru-6%Co/MSEP and 6%Co-6%CeO_2/MSEP catalysts the pore size was 3.0–4.0 nm, indicating that CeO_2 addition had no influence of the pore size distribution on the surface of catalysts.

From the FT-IR spectra of the catalysts (Fig. S3), the distinct peaks in all samples at 720 and 1020 cm^{-1} corresponded to the internal geminal Si—O bond and Si—O—Si bond, which were consistent with the result in the literature [24]. The peaks at 660 and 1610 cm^{-1} were attributed to the bending and stretching vibrations of O—H bond due to the abundant organic groups on MSEP surface. Weak peaks near 2350 cm^{-1} were attributed to the weak vibrations between metal species and oxygen element on the surface of catalyst, respectively.

From the XRD spectra of the catalysts (Fig. 1), MSEP exhibited characteristic diffraction peaks at $2\theta = 26.6°$, 50.1° and 68.3° [25], which were in accordance with our previous works [24]. The distinct diffraction peak at $2\theta = 44.2°$ were ascribed to the Ru(101) crystal (JCPDS 88-1734) [26]. The diffraction peaks at $2\theta = 42.3°$ and 76.1° were ascribed to the Co(111) and Co(200) crystal (JCPDS 01-1255) [27]. The characteristic diffraction peaks of CeO_2 were not observed, possibly due to their good dispersion on the surface of catalyst. The characteristic diffraction peaks of Ru and Co metals became weaker and dispersed better after CeO_2 species was added to the catalyst, which indicated that it promoted dispersion of Ru and Co metal atoms.

From the pyridine adsorbed FT-IR spectra of the samples (Fig. S4), the IR band at 1450 cm^{-1} is the adsorption of pyridine on Lewis acidic centers, the band at 1490 cm^{-1} is the interaction of pyridine with Lewis and Brønsted acid sites, and the band at 1540 cm^{-1} is the adsorption of pyridine on Brønsted acid centers. The results indicate that MSEP possessed both Lewis and Brønsted acid sites, and CeO_2 increased the Brønsted acid sites, which had significant influence on the catalytic performance.

The SEM and TEM images of the studied catalyst are shown in Fig. 2. Where many white fibric states were unrolled unsymmetrical (Fig. 2a), the metal species were not distinguishable at ×20,000 magnification. As shown in Fig. 2b, many uniform flakes formed a large amount on hollow fabric channels and black dots due to metal atom as a result of the magnification, CeO_2 was observed at ×200,000 magnification. CeO_2 can be distinguished from Fig. 2c, and the metal atoms remained in the inner site of hollow fabric channels with good dispersion at ×400,000 magnification. Furthermore, due to the presence of abundant micro pore structures on the surface of catalyst, Ru and Co metal atoms at the inner site of pore were formed during the reduction process under a stream of pure H_2 (100 ml/min) at 723 K for 2 h. Under these conditions, aggregation could occur easily, but the addition of CeO_2 verted such issues and allowed metal atom dispersion, which was accordance with the literature data [16, 28]. Therefore, good dispersion of Ru and Co was achieved on the surface of MSEP in the presence of CeO_2.

The hydrogen chemisorption data of the studied catalysts are summarized in Table 2, in which 6%Ru-6%Co-6%CeO_2/MSEP demonstrated better dispersion, larger hydrogen uptake quantity and larger metal surface areas compared to the other catalysts. Co dispersion can be improved by 3.5% with addition of CeO_2 and the same change was performed for Ru/MSEP catalyst. For Ru-Co bimetallic catalysts, metal dispersion was improved by 6.1% with CeO_2. In the case of H_2 uptake, the metal surface area and dispersion were improved with CeO_2 addition due to inhibition of metal atom agglomeration during the reduction process with the stream of pure H_2 at high temperature. Hence, both Ru and Co metal dispersion efficiently improved with the addition of CeO_2, which was consistent with TEM results.

Catalytic hydrogenation performance

The effects of various catalysts on the conversion and the selective catalytic hydrogenation of furfural to CPO were examined under catalytic hydrogenation reaction condition at 433 K, with H_2 pressure of 3.0 MPa and reaction time of 6.0 h. Ru metal mass ratio of Ru/MSEP catalysts are shown in Fig. S5. 90% conversion of furfural was observed with Ru metal mass ratio of 6.0% in Ru/MSEP catalysts due to the high hydrogenation activity, but the selectivity to CPO and cyclopentanol production was only 30%, and the selectivity to furfuryl alcohol was approx. 25%. Other products detected included tetrahydro furfuryl alcohol, 1,2-pentanediol, 1,4-pentanediol, 1,2-cyclopentanediol and 1,3-cyclopentanediol. Considering the selectivity to major product is not ideal, another metal had been introduced and fixed the Ru metal mass ratio at 6%.

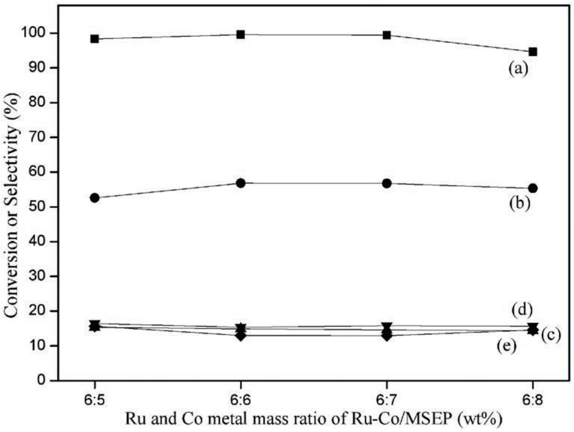

Fig. 3 Effects of Ru:Co metal mass ratio of Ru-Co/MSEP catalysts: (a) conversion of furfural, and selectivity to (b) cyclopentanone, (c) cyclopentanol, (d) furfuryl alcohol, (e) others.

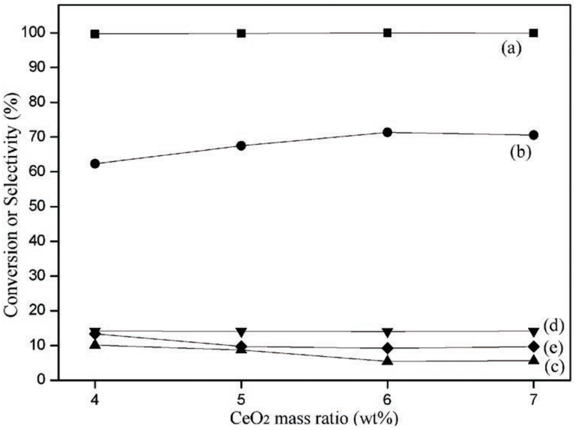

Fig. 4 Effects of CeO_2 mass ratio: (a) conversion of furfural, and selectivity to (b) cyclopentanone, (c) cyclopentanol, (d) furfuryl alcohol, (e) others.

From the influence of Co metal mass ratio of Co/MSEP catalysts as shown in Fig. S6 at the same reaction conditions, furfural conversion was below 50% at Co metal mass ratio of 8%. However, the selectivity to products produced was different from when using Ru/MSEP catalyst. Although the selectivity to CPO was low, the selectivity to cyclopentanol was approximately 5%, which indicated that Co metal could prevent hydrogenation of CPO to cyclopentanol. The selectivity to furfuryl alcohol was approximately 30% in the presence of Co/MSEP catalysts. Hence, Co/MSEP also was not sufficient.

Therefore, Ru-Co/MSEP bimetallic catalysts were

Table 3 Catalytic hydrogenation performance by some different catalysts.

Catalyst	Conversion (%)	Selectivity (%)			
		Cyclopentanone	Cyclopentanol	Furfuryl alcohol	Others*
6%Co/MSEP	42.38	34.59	3.65	31.14	30.62
6%Co-6%CeO_2/MSEP	40.21	43.31	5.65	35.14	15.90
6%Ru/MSEP	93.46	30.12	29.43	25.14	15.31
6%Ru-6%CeO_2/MSEP	86.45	36.31	29.37	24.99	9.33
6%Ru-6%Co/MSEP	99.56	56.82	14.89	15.33	12.96
6%Ru-6%Co-6%CeO_2/MSEP	100.00	71.35	5.42	13.99	9.24

Reaction conditions: temperature, 433 K; H_2 pressure, 3.0 MPa; time, 6.0 h; catalyst, 0.5 g.

* Others refers to tetrahydro furfuryl alcohol, 1,2-pentanediol, 1,4-pentanediol, 1,2-cyclopentanediol, and 1,3-cyclopentanediol, etc.

examined and the results are shown in Fig. 3 at the same reaction conditions. Ru metal mass ratio of Ru-Co/MSEP bimetallic catalysts was maintained at 6%, and the amount of Co metal was altered. The conversion of furfural was approximately 100%, which decreased as the amount of Co metal exceeded that of Ru metal. The selectivity to CPO was greater than 50% and that of cyclopentanol was below 15%. Hence, the selectivity to major product was better compared to singular metal catalysts. Both the selectivity to furfuryl alcohol and others was approximately 15%, therefore, the catalytic performance also improved.

The results for 6%Ru-6%Co-CeO_2/MSEP catalysts analysis (Fig. 4) with the same reaction conditions showed that the catalytic performance clearly improved. The conversion of furfural was approximately 100% in all cases and the selectivity to CPO reached 70% after addition of CeO_2. Cyclopentanol, selectivity was the lowest at 5.42% when the CeO_2 mass ratio of catalysts was 6%. The selectivity to furfuryl alcohol was 13.99% and to others was 9.24%. Depending on CeO_2 amount, the selectivity to CPO as major product was improved, then decreasing the formation of by-products.

In order to demonstrate the positive impact of CeO_2 in the studied catalysts, the catalytic hydrogenation results of various catalysts were compared and summarized in Table 3. Addition of CeO_2 to Co/MSEP or Ru/MSEP catalysts changed the selectivity ratio of products, where the selectivity to CPO was improved, where other decreased. However, the conversion of furfural did not improve due to some active sites on surface of catalyst being blocked by CeO_2 species. In the case of Ru-Co-CeO_2/MSEP catalysts, such trends were different. Ru and Co metals interacted each other during the reduction process by hydrogen stream and the active sites were enhanced. After addition of CeO_2, dispersion was enhanced, which was in accordance with TEM and hydrogen chemisorption results. CeO_2 species allowed excess of the hydrogenate inhibitor to Ru-Co bimetallic catalysts, as well as controlling the reaction channel of furfural hydrogenation for CPO production in water phase solution [29].

Table S1 shows the effects of reaction temperature on furfural hydrogenation over 6%Ru-6%Co-6%CeO_2/MSEP. It was clear that the reaction temperature significantly affected the catalytic performance. The conversion of furfural increased rapidly from 31.46% to 100.00% when the reaction temperature increased from 393 K to 433 K, and the selectivity to CPO increased from 68.41% to 71.35%. As the reaction temperature continued to rise, the selectivity to CPO began to decrease above 433 K. At the same time, higher reaction temperature promoted cyclopentanol formation, which caused more by-products. The effects of H_2 pressure on furfural hydrogenation over 6%Ru-6%Co-6%CeO_2/MSEP are shown in Table S2. The conversion of furfural was slightly altered when H_2 pressure increased from 2.2 MPa to 3.8 MPa. The selectivity to CPO was highest at H_2 pressure of 3.0 MPa, but excessive H_2 pressure favored cyclopentanol and other by-product production. The reaction temperature of 433 K and the H_2 pressure of 3.0 MPa were optimal conditions for the furfural hydrogenation to CPO over 6%Ru-6%Co-6%CeO_2/MSEP.

Examination of furfural initial concentration over 6%Ru-6%Co-6%CeO_2/MSEP catalyst is summarized in Table S3. The conversion of furfural stayed at 100.00% when the initial furfural concentration was below 5wt% in the water phase, but the conversion of furfural showed a clear decrease with the increment of the initial furfural concentration. The selectivity to cyclopentanone or cyclopentanol was close to 71% and 5.4%, respectively. If the initial furfural concentration reached 8.0% in water phase, other by-products were produced, including some unknown intermediate compounds in catalytic hydrogenation process.

The reusability of 6%Ru-6%Co-6%CeO_2/MSEP catalyst was investigated (Table S4). Typically, the catalysts were separated by filtration, washed and vacuum dried, and then reused. The catalytic performance slightly decreased until the fourth recycle, hence, the catatlyst could be easily recycled for this studied reaction. Furfural conversion decreased to 90.34%, and the selectivity to CPO decreased to 62.14% after the fifth cycle. Additionally, the selectivity to furfuryl alcohol and others increased with increasing cycles.

Considering that certain deactivation processes of the catalyst could be hindered at full conversion, additional experiments were conducted at low conversion level. The recycling of 6%Ru-6%Co-6%CeO_2/MSEP catalyst at low conversion level is shown in Table S5. The similar phenomenon has also existed since the reaction temperature had been chosen as 393 K. The furfural conversion decreased to 25.47%, and the selectivity to CPO decreased to 61.30% after the fifth cycle. Furthermore, the selectivity to furfuryl alcohol and other by-products increased with cycles. The conversion of furfural was low at low temperature, but the reusability of 6%Ru-6%Co-6%CeO_2/MSEP catalyst was also good.

In order to investigate the reason for deactivation reason after the fifth cycle, the spent catalyst was analyzed by XRD and TG. The peak signal of the spent catalyst showed an obvious change, where the characteristic diffraction peaks of Co(111) crystal ($2\theta = 42.3°$) and Co(200) crystal ($2\theta = 76.1°$) were sharper compared to the fresh catalyst (Fig. S7). Additionally, the diffraction peaks of MSEP became weaker, but the characteristic diffraction peak of Ru(101) crystal ($2\theta = 44.2°$) remained unchanged. Therefore, deactivation of Co metal atom is occurred easily in the water solution, where MSEP adsorbed water and the crystal form might change. TG curves (Fig. S8) revealed the different stages of the spent catalyst (Fig. S8a). The initial decomposition stage (160–220 °C) had a weight loss rate of approximately 2.93% due to the physisorption of water. Major degradation (19.81%) appeared in the second stage at 240–380 °C, which may be attributed to the phase transition of Co and CeO_2. The apparent degradation (29.76%) in the third stage at 450–700 °C may be attributed to the decomposition of MSEP. As shown in Fig. S8, TG curves of fresh 6%Ru-6%Co-6%CeO_2/MSEP catalyst revealed that the weight loss was only 3.60%, which suggested good thermal stability. The deactivation of the catalyst was ascribed to the crystallization of Co metal atoms and the phase transition of Co and CeO_2, hence, the reproducibility of the catalyst was limited.

The effects of solvent on the catalytic hydrogenation process of furfural were also studied. We selected ethanol, 1,4-dioxane, cyclohexane and heptane as the solvent, but the major product was furfuryl alcohol. Therefore, the water solution was very important for CPO production [30, 31], but a detailed reaction mechanism requires further investigations.

CONCLUSION

MSEP supported Ru-Co bimetallic catalysts were prepared by the impregnation method and applied in liquid phase furfural hydrogenation. The addition of CeO_2 species promoted the formation of smaller Ru and Co particles with better dispersion and more active sites for hydrogenation. CeO_2 increased the Brønsted acid sites of catalyst. Cleavage of the C=O bond in CPO could be prevented by Co metal and CeO_2, which enhanced CPO formation. 6%Ru-6%Co-6%CeO_2/MSEP catalyst gave the best catalytic performance of 71.35% selectivity to CPO, with good recycling capability and could be employed with 5.0 wt% initial furfural concentration (water as solvent). During the hydrogenation of furfural, cyclopentanol and furfuryl alcohol were the major by-products, with tetrahydro furfuryl alcohol, 1,2-pentanediol, 1,4-pentanediol, 1,2-cyclopentanediol and 1,3-cyclopentanediol in less amount. Further investigation is required to illustrate reaction mechanism.

Appendix A. Supplementary data

Supplementary data associated with this article can be found at http://dx.doi.org/10.2306/scienceasia1513-1874.2022.140.

Acknowledgements: This work was supported by Scientific Research Foundation for Advanced Talents of Guangdong University of Petrochemical Technology (2018rc50), Science and Technology Plan Project of Maoming city(2019395, 2021624), Open Fund of Guangdong Provincial Key Laboratory of Petrochemical Pollution Process and Control, Guangdong University of Petrochemical Technology (No. 2018B030322017) and 2021 University Students' Innovation and Entrepreneurship Training Program Project in Guangdong Higher Education (73321049).

REFERENCES

1. Liu S-J, Abrahamson LP, Scotta GM (2012) Biorefinery: ensuring biomass as a sustainable renewable source of chemicals, materials and energy. *Biomass Bioenerg* **39**, 1–4.
2. Mohan D, Pittman-Jr CU, Steele PH (2006) Pyrolysis of wood/biomass for bio-oil: a critical review. *Energy Fuel* **20**, 848–849.
3. Stöcker M (2008) Biofuels and biomass to liquid fuels in the biorefinery: catalytic conversion of lignocellulosic biomass using porous materials. *Angew Chem Int Ed* **47**, 9200–9211.
4. Kunkes EL, Simonetti DA, West RM, Serrano-Ruiz JC, Gärtner CA, Dumesic JA (2008) Catalytic conversion of biomass to monofunctional hydrocarbons and targeted liquid-fuel classes. *Science* **322**, 417–421.
5. Besson M, Gallezot P, Pinel C (2014) Conversion of biomass into chemicals over metal catalysts. *Chem Rev* **114**, 1827–1870.
6. Huber GW, Iborra S, Corma A (2006) Synthesis of transportation fuels from biomass: chemistry, catalysts, and engineering. *Chem Rev* **106**, 4044–4098.
7. Chanthon N, Ngaosuwan K, Kiatkittipong W, Wongsawaeng D, Appamana W, Assabumrungrat S (2021) A review of catalyst and multifunctional reactor development for sustainable biodiesel production. *ScienceAsia* **47**, 531–541.
8. Lange JP, Heide EVD, Buijtenen JV, Price R (2012) Furfural-a promising for lignocellulosic biofuels. *ChemSusChem* **5**, 150–166.

9. Li J-Q (2001) The chemistry and technology of furfural and its many by-products. *Chem Eng J* **81**, 338–339.
10. Stevens JG, Bourne RA, Twigg MV, Poliakoff M (2010) Real-time product switching using a twin catalyst system for the hydrogenation of furfural in supercritical CO_2. *Angew Chem Int Ed* **49**, 8856–8859.
11. Jean L, Morin J-F, Wehrung J-F, Magnin D, Chornet E (2010) High yield conversion of residual pentoses into furfural via zeolite catalysis and catalytic hydrogenation of furfural to 2-methylfuran. *Top Catal* **53**, 1231–1234.
12. Li X-L, Deng J, Shi J, Pan T, Yu C-G, Xu H-J, Fu Y (2015) Selective conversion of furfural to cyclopentanone or cyclopentanol using different preparation methods of Cu-Co catalysts. *Green Chem* **17**, 1038–1046.
13. Wang Y, Zhou M-H, Wang T-Z, Xiao G-M (2015) Conversion of furfural to cyclopentanol on Cu/Zn/Al catalysts derived from hydrotalcite-like materials. *Catal Lett* **145**, 1557–1565.
14. Wang Y, Sang S, Zhu W, Gao L, Xiao G (2016) CuNi@C catalysts with high activity derived from metal-organic frameworks precursor for conversion of furfural to cyclopentanone. *Chem Eng J* **299**, 104–111.
15. Hronec M, Fulajtárova K, Mičušik M (2013) Influence of furanic polymers on selectivity to furfural rearrangement to cyclopentanone. *Appl Catal A Gen* **468**, 426–431.
16. Zhang C, Lai Q-H, Holles J-H (2017) Bimetallic overlayer catalysts with high selectivity and reactivity for furfural hydrogenation. *Catal Commun* **89**, 77–80.
17. Yang Y-L, Du Z-T, Huang Y-Z, Lu F, Wang F, Gao J, Xu J (2013) Conversion of furfural into cyclopentanone over Ni-Cu bimetallic catalysts. *Green Chem* **15**, 1932–1940.
18. Hronec M, Fulajtá K, Vávra I, Soták T, Dobročka E, Mičušík M (2016) Carbon supported Pd-Cu catalysts for highly selective rearrangement of furfural to cyclopentanone. *Appl Catal B Environ* **181**, 210–219.
19. Zhu H-Y, Zhou M-H, Zeng Z, Xiao G-M, Xiao R (2014) Selective hydrogenation of furfural to cyclopentanone over Cu-Ni-Al hydrotalcite-based catalysts. *Korean J Chem Eng* **31**, 593–597.
20. Hronec M, Fulajtarová K (2012) Selective transformation of furfural to cyclopentanone. *Catal Commun* **24**, 100–104.
21. Zhang S-J, Ma H, Sun Y-X, Liu X, Zhang M-Y, Luo Y, Gao J, Xu J (2021) Selective tandem hydrogenation and rearrangement of furfural to cyclopentanone over CuNi bimetallic catalyst in water. *Chin J Catal* **42**, 2216–2224.
22. Li X-L, Zhu R (2022) A multi-functional porous cobalt catalyst for the selective hydrogenative ring-opening and rearrangement of furfural to cyclopentanol. *Mater Adv* **3**, 3855–3867.
23. Li X, Tong Z-K, Zhu S, Deng Q, Chen S-X, Wang J, Zeng Z-L, Zhang Y-L, et al (2022) Water-mediated hydrogen spillover accelerates hydrogenative ring-rearrangement of furfurals to cyclic compounds. *J Catal* **405**, 363–372.
24. Long W, Hao F, Xiong W, Liu PL, Luo H-A (2017) Modified sepiolite supported nickel and tungsten oxide catalysts for glycerol hydrogenolysis to 1,2-propanediol with high selectivity under mild conditions, *React Kinet Mech Cat* **122**, 85–100.
25. Tuler FE, Portela R, Aávila P, Banús ED, Miró EE, Milt VE (2015) Structured catalysts based on sepiolite with tailored porosity to remove diesel soot. *Appl Cata A Gen* **498**, 41–53.
26. Ishikawa M, Tamura M, Nakagawa Y, Tomishige K (2016) Demethoxylation of guaiacol and methoxy benzenes over carbon supported Ru-Mn catalyst. *Appl Catal B: environ* **182**, 193–203.
27. Ma Y-F, Wang H, Xu G-Y, Zhang Y, Fu Y (2017) Selective conversion of furfural to cyclopen-tanol over cobalt catalysts in on step. *Chin Chem Lett* **28**, 11153–1158.
28. Dutta G, Waghmare UV, Baidya T, Hegde M (2007) Hydrogen spillover on Pt/CeO_2: enhanced storage of active hydrogen. *Chem Mater* **19**, 6430–6436.
29. Pirmoradi M, Kastner JR (2021) A kinetic model of multi-step furfural hydrogenation over a $Pd-TiO_2$ supported activated carbon catalyst. *Chem Eng J* **414**, 128693–128703.
30. Li F, Jiang S-S, Wang Y, Huang J, Li C-Q (2021) Catalytic transfer hydrogenation of furfural over CuNi@C catalyst prepared from Cu-Ni metal-organic frameworks. *Russ J Phys Chem A* **95**, 68–79.
31. Hronec M, Fulajtarová K, Liptaj T (2012) Effect of catalyst and solvent on the furan ring rearrangement to cyclopentanone. *Appl Cata A Gen* **437–438**, 104–111.

Appendix A. Supplementary data

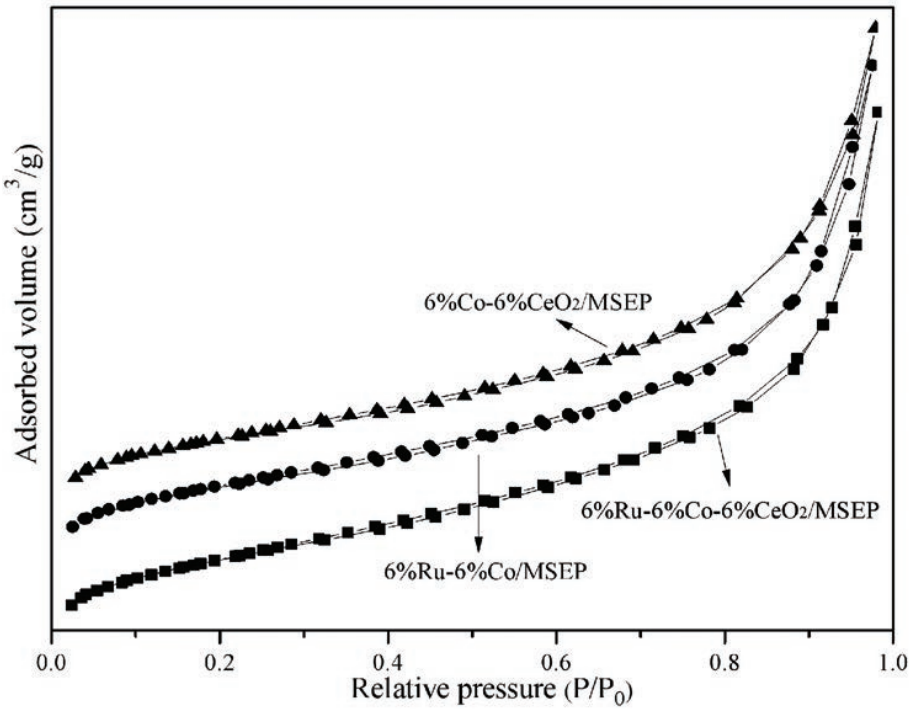

Fig. S1 N_2 adsorption/desorption isotherms of different samples.

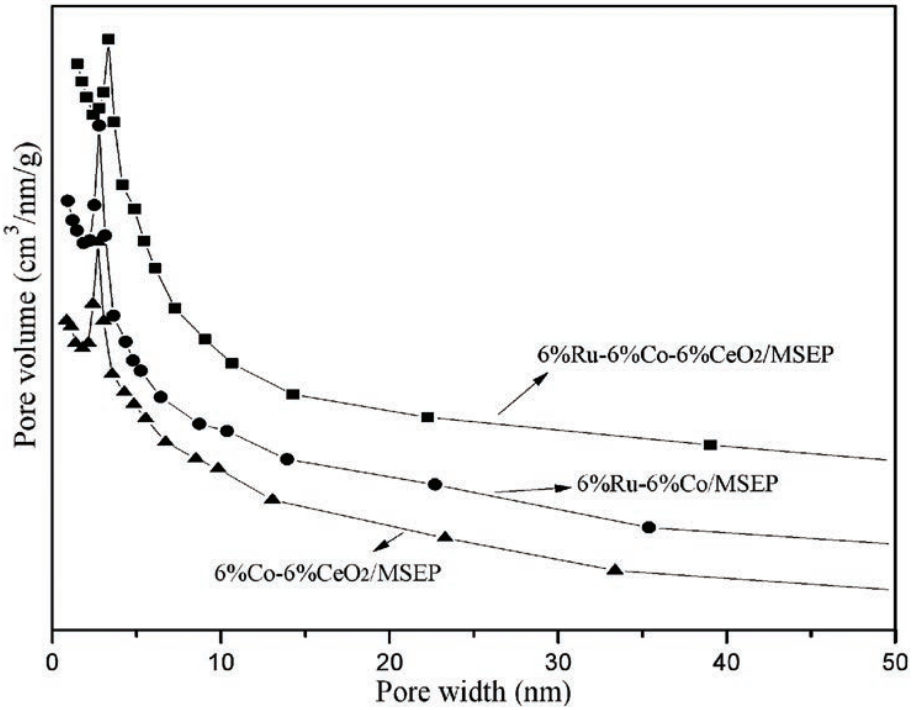

Fig. S2 The BJH pore size distributions of different samples.

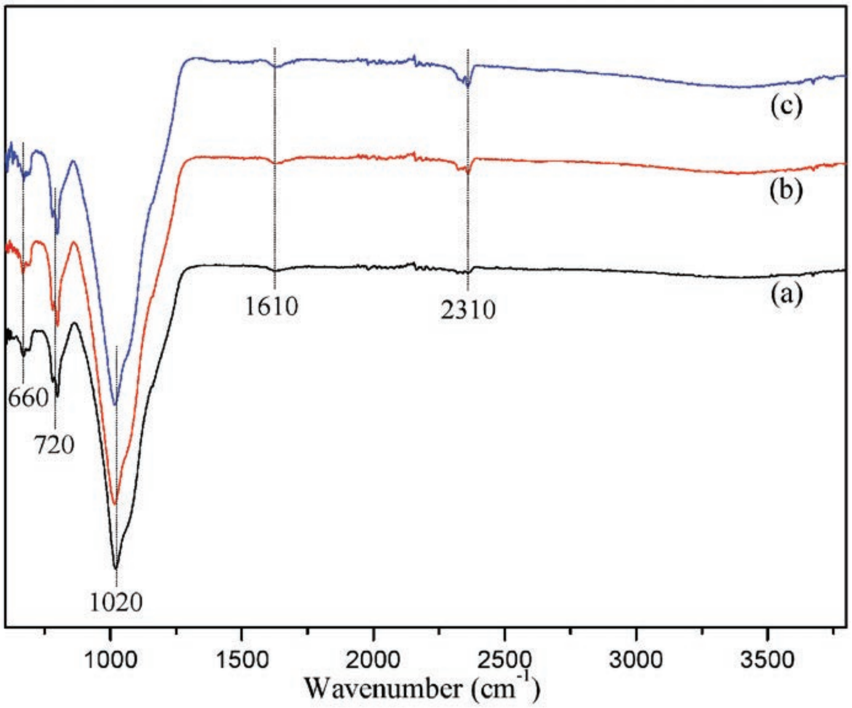

Fig. S3 FT-IR spectra of catalysts: (a) 6%Ru-6%Co-6%CeO_2/MSEP, (b) 6%Ru-6%Co/MSEP, (c) 6%Co-6%CeO_2/MSEP.

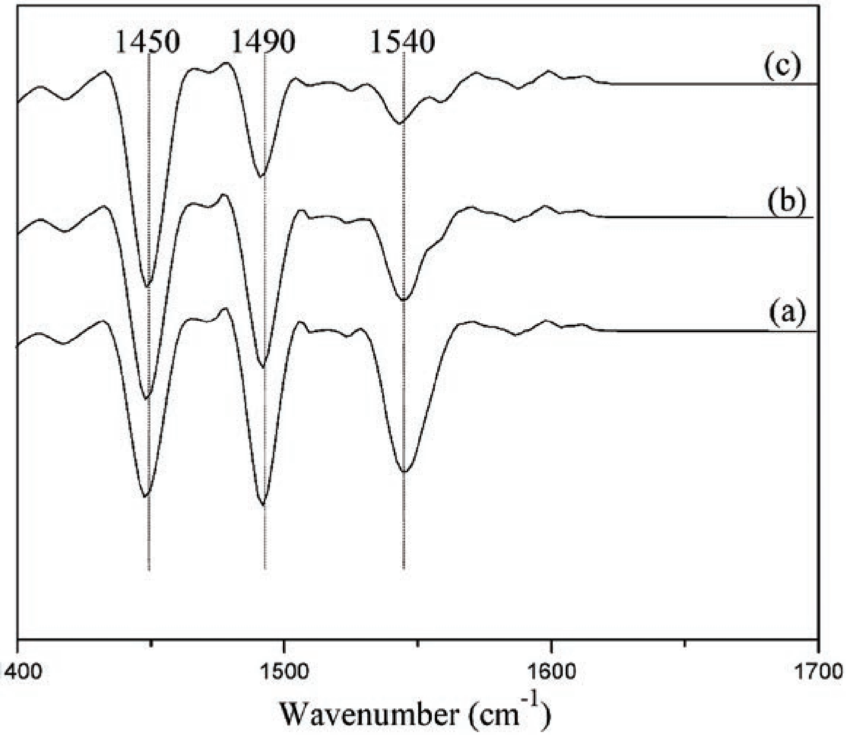

Fig. S4 Pyridine adsorbed FT-IR spectra of samples: (a) 6%Ru-6%Co-6%CeO_2/MSEP, (b) 6%Co-6%CeO_2/MSEP, (c) 6%Ru-6%Co/MSEP.

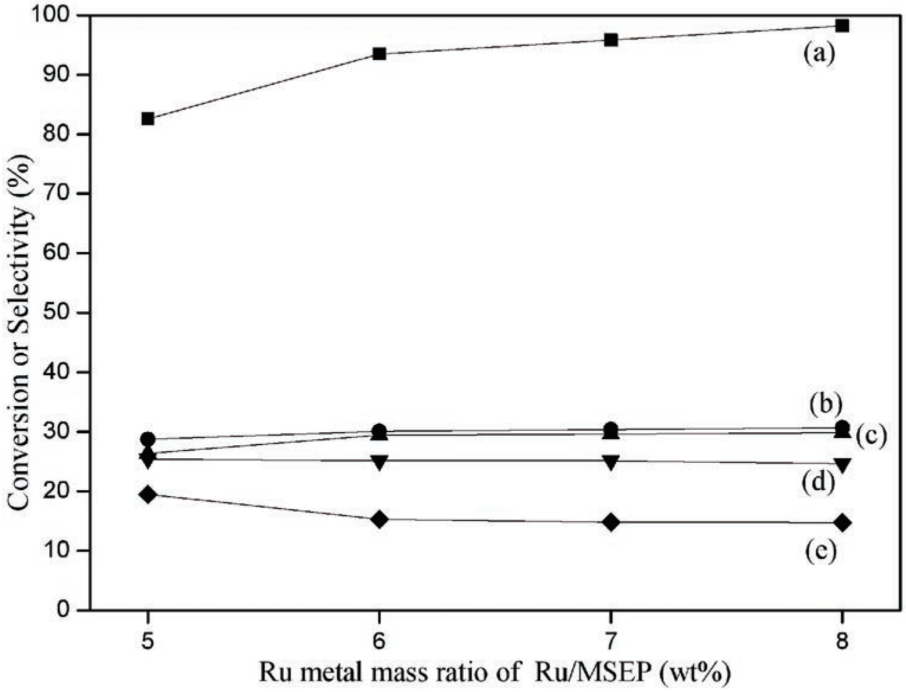

Fig. S5 Effects of Ru metal mass ratio of Ru/MSEP catalysts: (a) conversion of furfural, and selectivity to (b) cyclopentanone, (c) cyclopentanol, (d) furfuryl alcohol, (e) others.

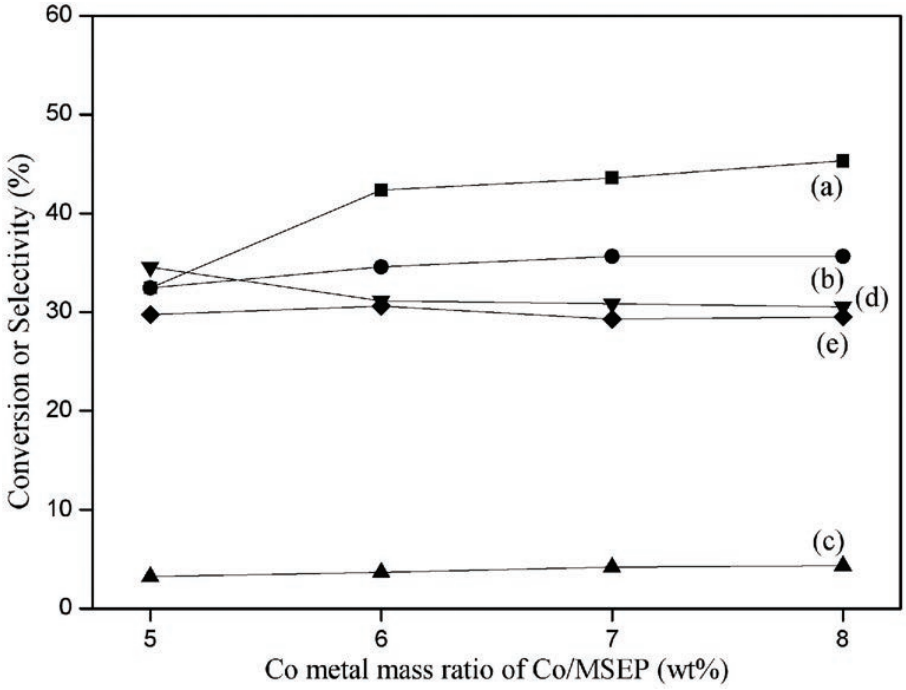

Fig. S6 Effects of Co metal mass ratio of Co/MSEP catalysts: (a) conversion of furfural, and selectivity to (b) cyclopentanone, (c) cyclopentanol, (d) furfuryl alcohol, (e) others.

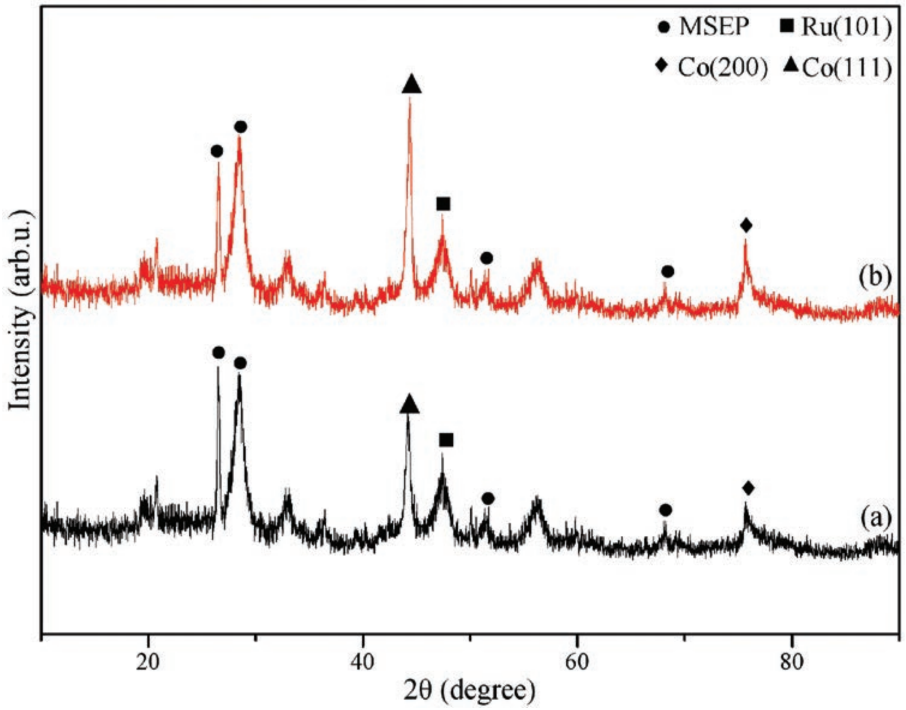

Fig. S7 X-ray diffraction(XRD) patterns of 6%Ru-6%Co-6%CeO_2/MSEP catalyst. (a) Fresh catalyst, (b) after the fifth cycle.

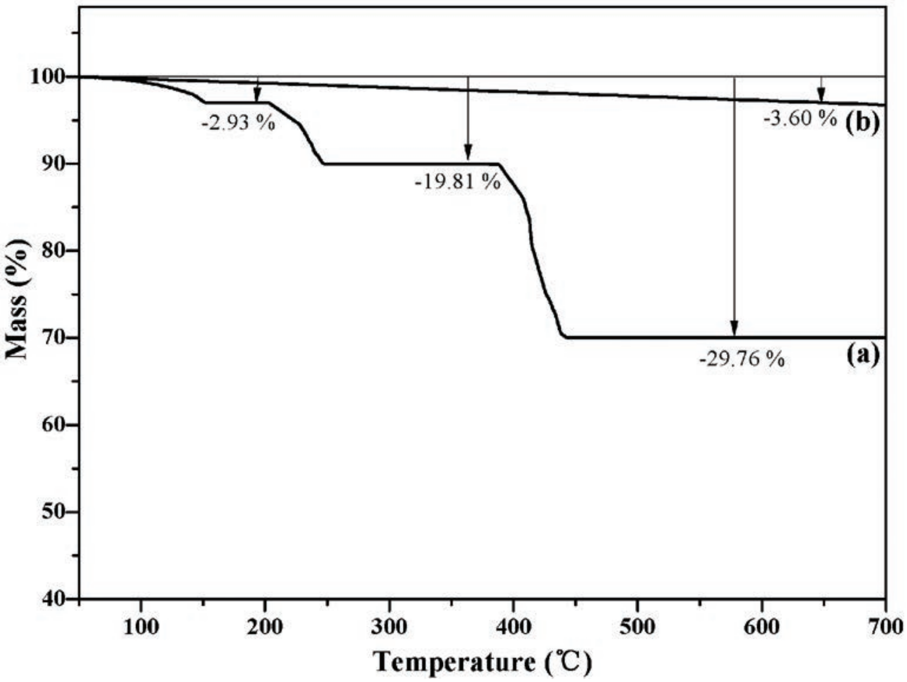

Fig. S8 TG curves of 6%Ru-6%Co-6%CeO_2/MSEP catalyst. (a) After the fifth cycle, (b) fresh catalyst.

Table S1 Effects of the reaction temperature.

Temperature (K)	Conversion (%)	Selectivity (%)			
		Cyclopentanone	Cyclopentanol	Furfuryl alcohol	Others*
393	31.46	68.41	4.86	17.69	9.04
403	42.68	69.72	5.02	16.87	8.39
413	63.79	70.35	5.16	15.37	9.12
423	89.74	70.56	5.37	14.23	9.84
433	100.00	71.35	5.42	13.99	9.24
443	100.00	70.88	5.79	14.21	9.12
453	100.00	69.84	6.31	14.89	8.96
463	100.00	67.33	8.47	15.13	9.07
473	100.00	62.19	11.32	15.47	11.02

Reaction conditions: H_2 pressure, 3.0 MPa; time, 6.0 h; catalyst, 6%Ru-6%Co-6%CeO_2/MSEP (0.5 g).

* Others refers to tetrahydro furfuryl alcohol, 1,2-pentanediol, 1,4-pentanediol, 1,2-cyclopentanediol, and 1,3-cyclopentanediol, etc.

Table S2 Effects of H_2 pressure.

H_2 pressure (MPa)	Conversion (%)	Selectivity (%)			
		Cyclopentanone	Cyclopentanol	Furfuryl alcohol	Others*
2.2	97.21	69.73	4.86	16.07	9.34
2.4	99.53	70.68	5.14	15.16	9.02
2.6	99.86	71.02	5.21	14.68	9.09
2.8	100.00	71.16	5.33	14.13	9.38
3.0	100.00	71.35	5.42	13.99	9.24
3.2	100.00	70.89	5.97	13.87	9.27
3.4	100.00	70.13	6.12	13.76	9.99
3.6	100.00	69.21	6.69	13.64	10.46
3.8	100.00	67.33	8.12	13.38	11.17

Reaction conditions: temperature, 433 K; time, 6.0 h; catalyst, 6%Ru-6%Co-6%CeO_2/MSEP (0.5 g).

* Others refers to tetrahydro furfuryl alcohol, 1,2-pentanediol, 1,4-pentanediol, 1,2-cyclopentanediol, and 1,3-cyclopentanediol, etc.

Table S3 Effects of initial furfural concentration over 6%Ru-6%Co-6%CeO_2/MSEP catalyst.

Initial furfural concentration (wt%)	Conversion (%)	Selectivity (%)			
		Cyclopentanone	Cyclopentanol	Furfuryl alcohol	Others*
3.0	100.00	70.69	5.86	15.31	8.14
4.0	100.00	71.07	5.73	14.26	8.94
5.0	100.00	71.35	5.42	13.99	9.24
6.0	98.41	71.35	5.42	14.06	9.17
7.0	95.27	70.67	5.43	15.13	8.77
8.0	87.33	69.85	5.42	15.24	10.49

Reaction conditions: temperature, 433 K; H_2 pressure, 3.0 MPa; time,6.0 h; catalyst, 0.5 g.

* Others refers to tetrahydro furfuryl alcohol, 1,2-pentanediol, 1,4-pentanediol, 1,2-cyclopentanediol, and 1,3-cyclopentanediol, etc.

Table S4 The cycle catalytic performance over 6%Ru-6%Co-6%CeO_2/MSEP catalyst.

Cycle order	Conversion (%)	Selectivity (%)			
		Cyclopentanone	Cyclopentanol	Furfuryl alcohol	Others*
1	100.00	71.35	5.42	13.99	9.24
2	100.00	71.35	5.43	14.00	9.22
3	99.34	71.25	5.43	14.11	9.21
4	98.71	71.07	5.40	14.30	9.23
5	90.34	62.14	5.28	18.93	13.65

Reaction conditions: temperature, 433 K; H_2 pressure, 3.0 MPa; time, 6.0 h; catalyst, 0.5 g.

* Others refers to tetrahydro furfuryl alcohol, 1,2-pentanediol, 1,4-pentanediol, 1,2-cyclopentanediol, and 1,3-cyclopentanediol, etc.

Table S5 The cycle catalytic performance over 6%Ru-6%Co-6%CeO_2/MSEP catalyst at low conversion level.

Cycle order	Conversion (%)	Selectivity (%)			
		Cyclopentanone	Cyclopentanol	Furfuryl alcohol	Others*
1	31.41	67.24	4.85	17.72	10.19
2	31.23	67.09	4.82	17.86	10.23
3	30.86	66.87	4.78	17.92	10.43
4	30.62	65.38	4.69	18.33	11.60
5	25.47	61.30	4.02	21.67	13.01

Reaction conditions: temperature, 393 K; time, 6.0 h; catalyst, 0.5 g.

* Others refers to tetrahydro furfuryl alcohol, 1,2-pentanediol, 1,4-pentanediol, 1,2-cyclopentanediol, and 1,3-cyclopentanediol, etc.